PAN
ARCHIVES OF ACOUSTICS
Vol. **45**, No. 3, pp. 377–384 (2020)
DOI: 10.24425/aoa.2020.134054

Research Paper

On a Robust Descriptor of the Flue Organ Pipe Transient

Viktor HRUŠKA*, Pavel DLASK

Academy of Performing Arts in Prague
Music Acoustics Research Centre
Prague, Czech Republic
*Corresponding Author e-mail: hruska.viktor@hamu.cz

(*received August 26, 2019; accepted March 12, 2020*)

The initial transient of an organ pipe is known to be of great influence to the perceived sound quality. At the same time, the unsteady process of the tone onset is essentially nonlinear and lacks exact repeatability, so the search for a robust descriptor is in place. Initial transients were recorded using an adjustable flue organ pipe. The blowing pressure and cut-up height were varied. Prony's method was employed to analyze the results. Utilizing the Principal Component Analysis (PCA) on the standardized exponential model coefficients, it was shown that the transients are well described by just one scalar parameter. Its value is predominantly dependent on the number of important Prony's components taking part in the transient process (i.e., the overall complexity of the transient signal). A strong correlation was found between the PCA component and the Strouhal number inverse.

Keywords: flue organ pipes; transient signal; Prony's method; Strouhal number.

1. Introduction

The initial transient of a flue organ pipe is known to be an essential source of tone quality differences, which makes it a subject of high relevance for research. Despite this fact, our knowledge of the process (in acoustical theory as well as the signal processing analysis) could be more profound and even establishing of a rough rule of thumb would be appreciated in organ building and pipe voicing applications. A nontrivial mixture of turbulence-induced noise, a build-up of future steady-state harmonics and tones supported by direct hydrodynamic feedback (whistle tones, mouth tones, aeolian tones, edge tones among other names) should be expected (Fabre, 2016; Außerlechner *et al.*, 2009).

State of the art aeroacoustics of fluid-structure interactions is unable to analytically predict the transient features, at least not unless substantial simplifications (Fabre, 2016). Experimental approaches employing the Particle Image Velocimetry or similar techniques (Yoshikawa *et al.*, 2012; Mickiewicz, 2015; Hruška, Dlask, 2017; 2019) show important connections between the pipe hydrodynamics and sound features but their description gives only rough outlines of the sounding far-field spectrum, not to mention that there is only a very limited amount of observations during the transient (Verge *et al.*, 1994; Yoshikawa, 2000). The Direct Numerical Simulations (Miyamoto *et al.*, 2013; Yokoyama *et al.*, 2015) are of growing importance, but since the computations are very costly even with the Large Eddy Simulation, it is not a method of wide practical use so far. The lumped-element models usually assume a steady-state operation in order to introduce a stable feedback loop (Dequand *et al.*, 2003; Fabre, Hirschberg, 2000). Some interesting results were brought by making use of the nonlinear dynamical systems theory (e.g., (Fischer *et al.*, 2016)), including the classical work on the flue organ pipe transient by Fletcher (1976).

This work focuses on the experimental approach and its signal processing connotations. A good deal of work has been done on the subject (Rioux, 2000; 2001; Angster, Miklós, 2000; Angster *et al.*, 2012; Taesch *et al.*, 2004; Nolle, Finch, 1992; Kob, 2010) using conventional frequency domain approach to isolate typical sound features. However, the spectral description making use of spectrograms have a major drawback. Its outcome is highly dependent on the algorithm parameters (such as the window length gov-

erning the time/frequency resolution). We are introducing a more holistic approach allowing for simple and efficient parameter count reduction based on the Prony's method. The method has been introduced to the field of music acoustics before (cf. Matrix-Pencil and ESPRIT algorithms as well), especially in the physically quite different context of idiophones and string vibrations (Laroche, 1993; Carrou *et al.*, 2009; Boutillon, David, 2002; Thomas *et al.*, 2003; Chaigne, Lambourg, 2001; Taillard *et al.*, 2018). Nevertheless, its application in the time-domain analysis of an aerophone signal, as presented below, is original.

The paper is organized as follows. First, the Prony's method (cf. (Marple, 1987) is reviewed, the transient detection procedure introduced (Sec. 2) and the measurement setup defined (Sec. 2). The results (Sec. 4) shows the outcome of Prony's method, along with some necessary restrictions arising from the decomposition qualities. Finally, the discussion and some conclusions are given (Secs 5 and 6).

2. Methods

2.1. The Prony's method

The Prony's method decomposes a signal consisting of N samples $\boldsymbol{x} = \{x_0, x_1, ..., x_{N-1}\}$ into a sum of complex exponentials (Marple, 1987). More precisely, it fits following exponential model in a least squares sense

$$\widehat{x}_n = \sum_{k=1}^{p} A_k e^{(\alpha_k + i2\pi f_k)(n-1)T + i\phi_k} = \sum_{k=1}^{p} h_k z_k^{n-1}, \tag{1}$$

where $h_k \equiv A_k e^{i\phi_k}$ and $z_k \equiv e^{(\alpha_k + i2\pi f_k)T}$. A_k, α_k, f_k, ϕ_k are the amplitude, damping coefficient, frequency and initial phase of the k-th mode respectively. An inverse of T is the sampling frequency. The value of p is the polynomial order of linear prediction used in the method (see below). It is defined as 11/12 of maximal order, which is given as half of the signal length (in samples).

A sequence of three steps is usually described when the method is introduced. First, the linear prediction model is computed

$$\begin{bmatrix} x_p \\ x_{p+1} \\ \vdots \\ x_{N-1} \end{bmatrix} = \begin{bmatrix} x_{p-1} & x_{p-2} & \cdots & x_0 \\ x_p & x_{p-1} & \cdots & x_1 \\ \vdots & \vdots & \ddots & \vdots \\ x_{N-2} & x_{N-3} & \cdots & x_{N-p-1} \end{bmatrix} \begin{bmatrix} a_1 \\ a_2 \\ \vdots \\ a_p \end{bmatrix}, \tag{2}$$

where $\boldsymbol{a}$ is the parameter vector and the matrix is of Toeplitz type. The Eq (2) is solved for $\widehat{\boldsymbol{a}}$ using the Moore-Penrose matrix pseudo-inverse (for a matrix $\mathbf{B}$, the pseudo-inverse $\mathbf{B}^+$ is given as $\mathbf{B}^+ \equiv \left(\mathbf{B}^{\mathrm{H}}\mathbf{B}\right)^{-1}\mathbf{B}^{\mathrm{H}}$, where $(\ )^{\mathrm{H}}$ denotes the Hermitian transpose).

In the second step, the values of z are obtained as the roots of the characteristic polynomial

$$z^p - \left(a_1 z^{p-1} + a_2 z^{p-2} + ... + a_p z^0\right) = 0. \tag{3}$$

The roots $\boldsymbol{z}$ are discrete-time $\mathcal{Z}$-domain approximation of continuous-time eigenvalues. The damping ratio α_k and frequency f_k are then calculated as

$$\alpha_k = \frac{1}{T}\ln|z_k|, \tag{4}$$

$$f_k = \tan^{-1}\frac{\Re\{z_k\}}{\Im\{z_k\}}. \tag{5}$$

The last step consists of modal amplitudes and initial phases computation using a linear regression model

$$\begin{bmatrix} x_0 \\ x_1 \\ \vdots \\ x_{N-1} \end{bmatrix} = \begin{bmatrix} 1 & 1 & \cdots & 1 \\ z_1^1 & z_2^1 & \cdots & z_p^1 \\ \vdots & \vdots & \ddots & \vdots \\ z_1^{N-1} & z_2^{N-1} & \cdots & z_p^{N-1} \end{bmatrix} \begin{bmatrix} h_1 \\ h_2 \\ \vdots \\ h_p \end{bmatrix}, \tag{6}$$

where the matrix is of Vandermonde type. The $\widehat{\boldsymbol{h}}$ is again obtained by matrix pseudo-inverse and consequently the amplitudes and phases are calculated:

$$A_k = |h_k|, \tag{7}$$

$$f_k = \tan^{-1}\frac{\Re\{h_k\}}{\Im\{h_k\}}. \tag{8}$$

Since the Prony's method on high-resolution signals is computationally very costly, the signals were downsampled before the computation. The downsampling took place after the zero-phase anti-aliasing lowpass Butterworth filter had been applied.

The performance of the algorithm is better when the decomposed signals have not the initial amplitudes close to zero (i.e., when the signal is fading out, not building up). Therefore the initial transients were decomposed in reversed time. Note that it does not influence the interpretation of the results given below in any manner.

The algorithm was implemented in GNU Octave using its built-in functions (`pinv`, `roots`, `butter` etc.).

2.2. Transient detection

In experimental practice, there is no possibility of obtaining a perfect steady-state of the sound signal and consequently distinguish the transient part as a remainder. We shall come up with an appropriate way of the transient detection that is close enough to the abstract ideal case and make use of it despite inevitable imperfections.

We suppose that our signals are long enough to reach the steady-state in the first place. The recording

started at the keystroke and lasts over 0.5 s. Since the periodicity is one of the essential traits of the steady-state, we begin with it. By means of autocorrelation, we obtain the duration of one period and divide the whole signal into parts of its length. Next, we calculate the fast Fourier transform (FFT) of each part and focus on the first three coefficients (i.e., the first three harmonics, because the FFT window is of exactly one period in length).

We assume that the last quarter of the signal (ca. 0.4 s after the keystroke) is steady-state. Hence, we have the steady values of the first three harmonics. However, the "steady-state" exhibits non-negligible fluctuations in many voicing setups. We adjust our definition accordingly. The signal is investigated backward, i.e., starting in the assumed steady-state and receding to the presumed transient. We define that the signal segment is not of the steady-state any more if any of the three harmonics reach a value that is not within 6 standard deviations σ of its steady-state value.

On the other hand, a starting point of the transient is much easier to be found. We define that the signal segment is already a sound signal of interest if its power is at least 0.1% of the mean steady-state period power.

The introduced method is summarized in Fig. 1 and an example is depicted in Fig. 2.

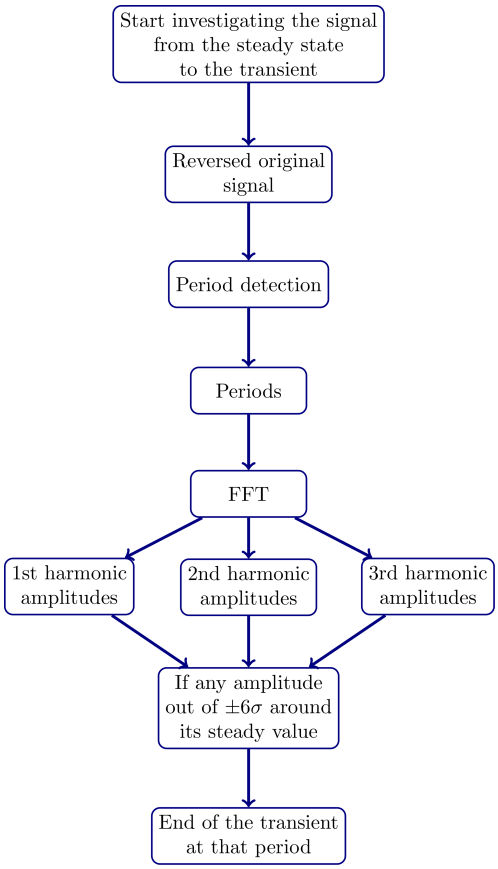

Fig. 1. Block diagram of the transient detection procedure.

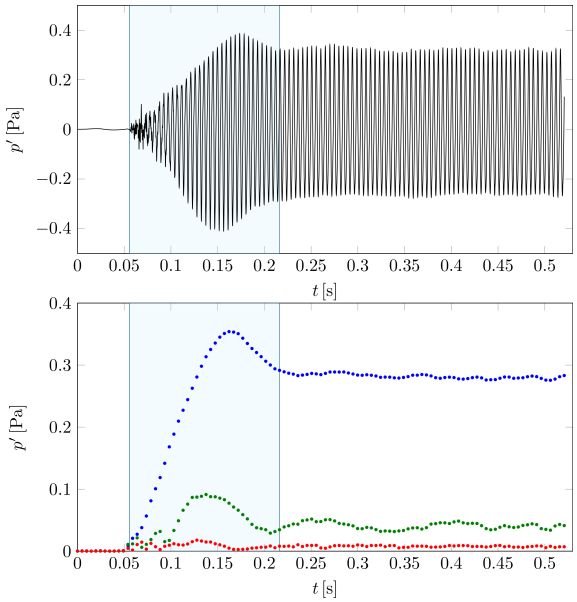

Fig. 2. Example of the transient detection procedure. Top: the analysed signal, bottom: the values of the three harmonics amplitudes (1st – blue, 2nd – green, 3rd – red). In the background the timespan of the transient is marked.

3. Measurement

A rectangular plexiglass open flue organ pipe of fundamental frequency 207 Hz was used for measurements (Fig. 4). The cut-up height W was adjustable by shifting the languid (or "the block" in rectangular organ pipes) and ranged from 9 to 26 mm during the experiment (Fig. 3). The organ pipe was attached

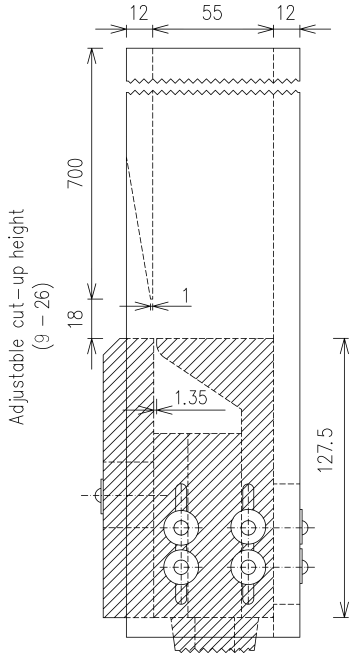

Fig. 3. Drawing of the adjustable flue organ pipe. The values are in milimeters.

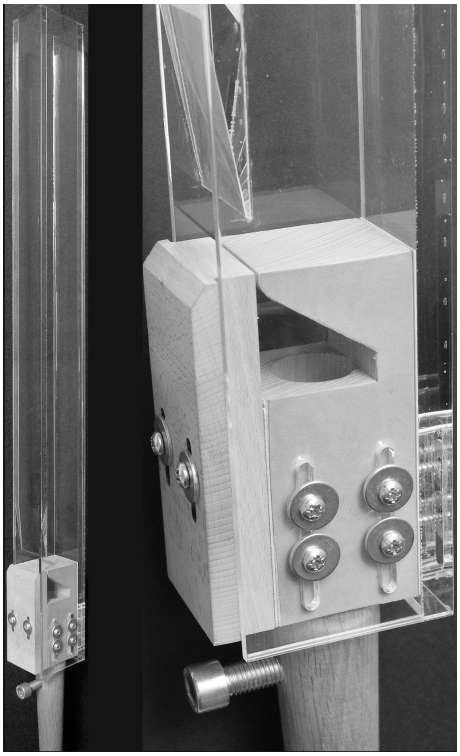

Fig. 4. The experimental flue organ pipe and detail of its mouth region.

to a small laboratory windchest with a curtain valve mechanism to maintain a constant blowing pressure. Since the pressure control screw was placed at the foot entrance, the actual blowing pressure inside the foot was measured above it. The foot (over-)pressure p_f ranged from 35 to 150 Pa, and it was used to assess the jet velocity U_{jet} according to the Bernoulli's formula given that the air velocity just above the screw is small compared to the flue velocity

$$U_{\text{jet}} = \sqrt{\frac{2p_f}{\rho_0}}, \tag{9}$$

where ρ_0 denotes the ambient air density.

The set-up labeled by the organ-builder as the pipe optimum (based on his craftsman experience and sensation) was $W = 18$ mm, $p_f = 86$ Pa. The flue width h was 1.35 mm, which gives an estimate of the Reynolds number $\text{Re} = U_{\text{jet}}h/\nu$ between 800 and 1700 (ν denotes the kinematic viscosity of air). The W/h ratio was approximately 8–19.

Sound recordings took place in an anechoic chamber. Five takes were recorded are further treated by the $W-p_f$ setup (in order to asses the uncertainty given by the bad repeatability). There was at least 10 s break between the takes to assure that the inertial effects inside the pipe ceased. The microphone was placed 2 m from the pipe axis. The original 192 kHz sampling rate was downsampled to 12 kHz for the Prony's method computation.

4. Results

The transient signals were described by the three most important Prony's components (i.e., 3 pairs of components with the complex argument of the exponent). A simple rule assessed the component importance: the most important mode minimizes the power of the residual signal (the Prony's component subtracted from the original signal), the second one minimizes this residuum in the same manner and so on. The fit was deemed satisfactory if the three components contain over 80% of the transient signal power. The relative powers of the residual signals left were recorded for each component. For the reader's convenience, further treatment is summarized in a block diagram in Fig. 5.

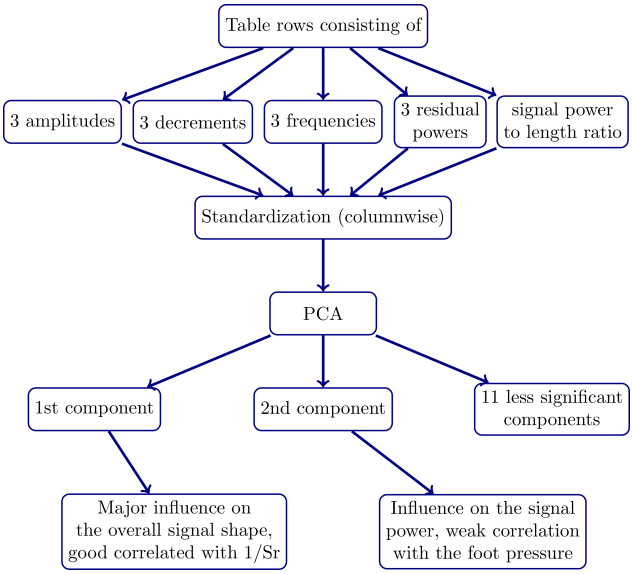

Fig. 5. Block diagram summarizing the treatment of the results.

The previous steps result in a representation of a transient signal with a vector consisting of 3 component frequencies, 3 component damping factors, 3 residual signal powers and a ratio of the total power of the signal and its length was added as the 13th component. Subsequently, all the vector components were standardized over all recordings (i.e., the mean value of component was subtracted, and then all matching components were divided by their standard deviation).

So far, the information from each of the recordings was reduced to 13 vector components. The number of necessary parameters was further diminished by principal component analysis (PCA). As it is shown in Fig. 6, there is only one important mode explaining almost 30% of the variance.

The 1st PCA component score turned out to be represented by the overall complexity of the transient. Signals consisting of one characteristic frequency, a slow gradual attack leading directly to the steady-

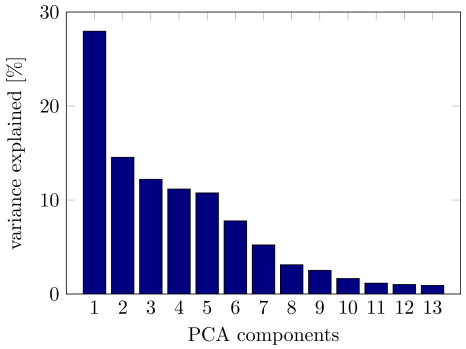

Fig. 6. Variance explained by the principal components.

state and with an abrupt fall of the residual power after just one or two Prony's components exhibit low values of the component score. On the other hand, signals of complicated attack, high frequency diversity, and several almost equally important Prony's components are labeled with high values of the 1st PCA component. For a better illustration, three characteristic signals, along with their Prony's components, are shown in Fig. 7. The first example on the left (low score) has the frequencies of all components in the vicinity of the 1st harmonic, and the 3rd Prony's component is already quite weak. On the other hand, the third example (high score) has all components of significant importance, and the first two have frequencies at the 2nd harmonic.

A significant correlation (0.79, p-value 0 to the machine precision) was found between the 1st PCA parameter and the Strouhal number inverse 1/Sr defined as

$$\frac{1}{\mathrm{Sr}} = \frac{U_{\mathrm{jet}}}{fW} = \frac{1}{fW}\sqrt{\frac{2p_f}{\rho_0}}, \tag{10}$$

where f denotes the pipe (acoustical) fundamental frequency $f = 207$ Hz.

It implicates that simple and smooth attack transient signals should be expected for the pipe and windchest setups leading to high Strouhal numbers (i.e., high cut-up and low blowing pressure) and conversely

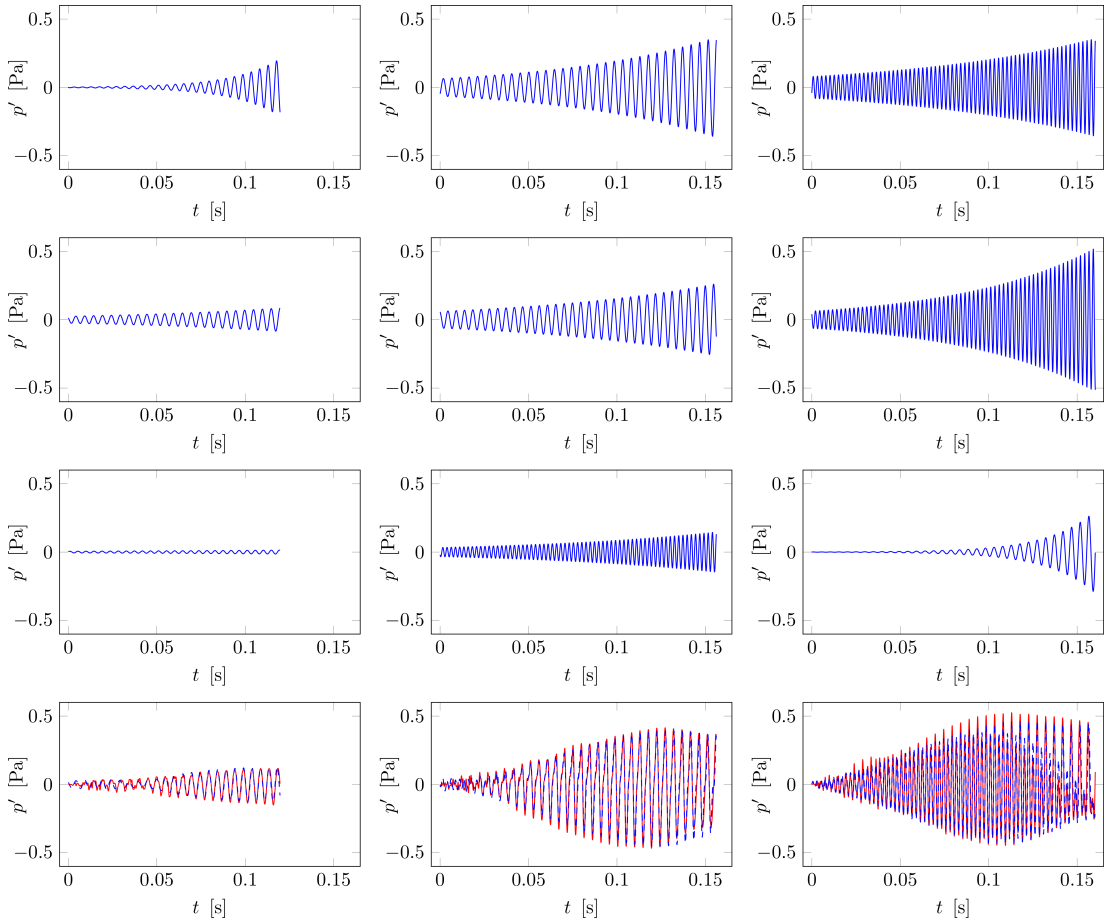

Fig. 7. Three examples corresponding to the low (left), middle (middle) and high (right) values of the 1st PCA component. In the last row the original signal (red) and sum of the 3 Prony's components (blue, dashed) is shown. The corresponding Prony's components are depicted in columns above (the most important in the first row and then in descending order). The cut-up height W and the foot pressure p_f were 17 mm – 36 Pa (left column), 18 mm – 101 Pa (middle column), 11 mm – 151 Pa (right column) [color online].

for small cut-ups and strong airflow. See the 1st PCA component score plotted against the 1/Sr in Fig. 8. Note, however, that very simple transient might not be the goal from the musical point of view. The dependence of the key features of the organ pipe sound on the Strouhal number is in accordance with the previous research on the internal amplitude of the acoustic field (Verge *et al.*, 1997).

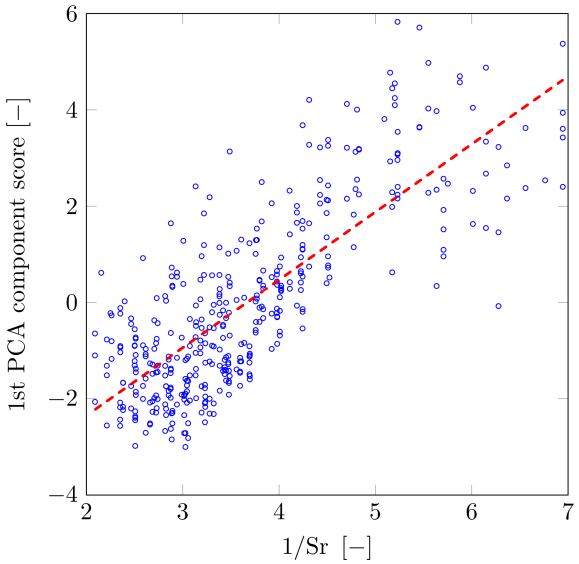

Fig. 8. The 1st PCA component score of the 411 transients plotted against the 1/Sr. A linear fit is indicated by the dashed line.

Although the 1st PCA component explains only 28% of the variance, the coefficient 1/Sr is probably the only one robust descriptor connecting the initial transient quality with the pipe set up. Note that the 1st component explains twice the variance compared to the 2nd one and the variance explained by the components apart from the 1st converges almost uniformly. The 2nd PCA component is primarily responsible for the total power in the signal, but it is only weakly correlated (0.48) with the foot pressure. No other significant correlations were found among the rest of the PCA components, even for basic nonlinear combinations of the voicing parameters. It might suggest that these modes decompose only a non-deterministic content of the total variance. Finally, given the well-known bad repeatability of the transients, the component explaining more than a quarter of the overall variance should not be deemed weak.

5. Discussion

The main goal of the following paragraphs is an estimation of effects due to the treatment parameters.

Since the mouth area was varied during the experiment, the length corrections might have been taken into account (cf. (Fletcher, Rossing, 1998)). However, their introduction changes neither the correlation values nor the interpretation of the results. If four or five Prony's components are used instead of three, the correlation coefficient of the 1st PCA component varies ± 0.03, and again, the interpretation remains unchanged.

The recordings took place not far from the pipe (2 m). Therefore the role of interference due to the mouth and the open end radiation cannot be excluded (cf. e.g., (Fabre, 2016)). Such issues are inevitable due to limited space in the anechoic chamber: it is not possible to reach the far-field of the quasi-dipole with 0.7 m separation of sources. In order to asses the influence of interference, the same procedure has been applied to smaller amounts of signals in different directions. Although the specific corresponding signals are obviously not identical, the overall trend and its implications stay the same.

The initial phases of the three most important Prony's components were not included in the analysis above as they had very little effect on the results. There was not any trend found among them.

The differences in the foot pressure build-up among the same voicing setups was measured. The magnitude of the differences was under 1% of the overpressure value.

There is no practical possibility of making the input parameters range denser or wider. The pipe failed to play or started to overblow for pressures and cut-up heights outside the presented matrix. The accuracy of the windchest pressure or cut-up heights cannot be assured for finer steps (e.g., cut-up height steps smaller than 1 mm). In other words, the correlations would be highly polluted by the input parameters uncertainties.

Naturally, from the introduced approach, any details of pipe mouth fluid dynamics cannot be directly assessed.

When more voicing parameters are varied (e.g., the flue width) the 1/Sr might not be the only descriptor needed.

Errors of the Prony's method due to outliers or non-gaussian noise were not observed so far. The conventional Prony's method was sufficient for the task (see, e.g., (Netto, Milli, 2017) for further discussion).

6. Conclusions

Prony's method has been used as a tool for the flue organ pipe transient analysis. By investigation of attack transients of different setups (cut-up height and blowing pressure), the robust descriptor of the waveform has been found, namely the quantity 1/Sr. The main differences among studied signals have been found in the overall complexity of the waveform – the number of important Prony's components taking part and variety of strong frequencies occurring during the transient (see Fig. 7).

The future research should focus on more sophisticated criteria based on which the important Prony's modes are chosen (Aguirre, 1993; Reynders *et al.*, 2012). The other logical direction is the generalization of the introduced $p_f - W$ parameter plane by more voicing parameters.

Acknowledgement

This publication was written at the Academy of Performing Arts in Prague as part of the project "Subjective and objective aspects of musical sound quality" with the support of the Institutional Endowment for the Long Term Conceptual Development of Research Institutes, as provided by the Ministry of Education, Youth and Sports of the Czech Republic.

References

1. Aguirre L. (1993), Quantitative measure of modal dominance for continuous systems, [in:] *Proceedings of 32nd IEEE Conference on Decision and Control*, Vol. 3, pp. 2405–2410, doi: 10.1109/CDC.1993.325629.
2. Angster J., Miklós A. (2000), Properties of the sound of flue organ pipes, *Acta Acustica united with Acustica*, **86**(4): 611–622.
3. Angster J., Miklós A., Rucz P., Augusztinovicz F. (2012), The physics and sound design of flue organ pipes, *The Journal of the Acoustical Society of America*, **132**(3): 2069–2069, doi: 10.1121/1.4755627.
4. Ausserlechner H.J., Trommer T., Angster J., Miklós A. (2009), Experimental jet velocity and edge tone investigations on a foot model of an organ pipe, *The Journal of the Acoustical Society of America*, **126**(2): 878–886, doi: 10.1121/1.3158935.
5. Boutillon X., David B. (2002), Assessing tuning and damping of historical carillon bells and their changes through restoration, *Applied Acoustics*, **63**(8): 901–910, doi: 10.1016/S0003-682X(01)00067-6.
6. Carrou J.-L.L., Gautier F., Badeau R. (2009), Sympathetic string modes in the concert harp, *Acta Acustica united with Acustica*, **95**(4): 744–752.
7. Chaigne A., Lambourg C. (2001), Time-domain simulation of damped impacted plates. I. Theory and experiments, *The Journal of the Acoustical Society of America*, **109**(4): 1422–1432, doi: 10.1121/1.1354200.
8. Dequand S. *et al.* (2003), Simplified models of flue instruments: influence of mouth geometry on the sound source, *Journal of Acoustical Society of America*, **113**(3): 1724–1735, doi: 10.1121/1.1543929.
9. Fabre B. (2016), Flute-like instruments, [in:] A. Chaigne, J. Kergomard, *Acoustics of Musical Instruments*, pp. 559–606, Springer, New York, NY, doi: 10.1007/978-1-4939-3679-3.
10. Fabre B., Hirschberg A. (2000), Physical modeling of flue instruments: A review of lumped models, *Acta Acustica united with Acustica*, **86**(4): 599–610.
11. Fischer J.L., Bader R., Abel M. (2016), Aeroacoustical coupling and synchronization of organ pipes, *The Journal of the Acoustical Society of America*, **140**(4): 2344–2351, doi: 10.1121/1.4964135.
12. Fletcher N., Rossing T. (1998), *The Physics of Musical Instruments*, Springer, New York.
13. Fletcher N.H. (1976), Transients in the speech of organ flue pipes – a theoretical study, *Acta Acustica united with Acustica*, **34**(4): 224–233.
14. Hruška V., Dlask P. (2017), Connections between organ pipe noise and shannon entropy of the airflow: Preliminary results, *Acta Acustica united with Acustica*, **103**(6): 1100–1105.
15. Hruška V., Dlask P. (2019), Investigation of the sound source regions in open and closed organ pipes, *Archives of Acoustics*, **44**(3): 467–474, doi: 10.24425/aoa.2019.129262.
16. Kob M. (2010), Influence of wall vibrations on the transient sound of flue organ pipes, *The Journal of the Acoustical Society of America*, **128**(4): 2419–2419, doi: 10.1121/1.3508635.
17. Laroche J. (1993), The use of the matrix pencil method for the spectrum analysis of musical signals, *The Journal of the Acoustical Society of America*, **94**(4): 1958–1965, doi: 10.1121/1.407519.
18. Marple S.L. (1987), *Digital Spectral Analysis: with Applications/Disk,Pc/MS Dos/IBM/Pc/at*, *Prentice Hall Signal Processing Series*, Prentice Hall.
19. Mickiewicz W. (2015), Particle image velocimetry and proper orthogonal decomposition applied to aerodynamic sound source region visualization in organ flue pipe, *Archives of Acoustics*, **40**(4): 475–484, doi: 10.1515/aoa-2015-0047.
20. Miyamoto M. *et al.* (2013), Numerical study on acoustic oscillations of 2d and 3d flue organ pipe like instruments with compressible LES, *Acta Acustica united with Acustica*, **99**(1): 154–171, doi: 10.3813/AAA.918599.
21. Netto M., Milli L. (2017), A robust prony method for power system electromechanical modes identification, [in:] *2017 IEEE Power and Energy Society General Meeting*, Chicago, IL, doi: 10.1109/PESGM.2017.8274323.
22. Nolle A.W., Finch T.L. (1992), Starting transients of flue organ pipes in relation to pressure rise time, *The Journal of the Acoustical Society of America*, **91**(4): 2190–2202, doi: 10.1121/1.403653.
23. Reynders E., Houbrechts J., Roeck G.D. (2012), Fully automated (operational) modal analysis, *Mechanical Systems and Signal Processing*, **29**: 228–250, doi: 10.1016/j.ymssp.2012.01.007.

24. Rioux V. (2000), Methods for an objective and subjective description of starting transients of some flue organ pipes – integrating the view of an organ-builder, *Acta Acustica united with Acustica*, **86**(4): 634–641.

25. Rioux V. (2001), *Sound quality of flue organ pipes*, PhD thesis, Chalmers University of Technology, Göteborg.

26. Taesch C., Wik T., Angster J., Miklós A. (2004), Attack transient analysis of flue organ pipes with different cut-up height, [in:] *Proceedings of CFA/DAGA*, Strasbourg.

27. Taillard P.-A., Silva F., Guillemain P., Kergomard J. (2018), Modal analysis of the input impedance of wind instruments, application to the sound synthesis of a clarinet, *Applied Acoustics*, **141**: 271–280, doi: 10.1016/j.apacoust.2018.07.018.

28. Thomas O., Touzé C., Chaigne A. (2003), Asymmetric non-linear forced vibrations of free-edge circular plates. Part II: Experiments, *Journal of Sound and Vibration*, **265**(5): 1075–1101, doi: 10.1016/S0022-460X(02)01564-X.

29. Verge M.-P., Fabre B., Hirschberg A., Wijnands A.P.J. (1997), Sound production in recorder-like instruments. I. Dimensionless amplitude of the internal acoustic field, *The Journal of the Acoustical Society of America*, **101**(5): 2914–2924, doi: 10.1121/1.418521.

30. Verge M.P. *et al.* (1994), Jet formation and jet velocity fluctuations in a flue organ pipe, *The Journal of the Acoustical Society of America*, **95**(2): 1119–1132, doi: 10.1121/1.408460.

31. Yokoyama H., Miki A., Onitsuka H., Iida A. (2015), Direct numerical simulation of fluid–acoustic interactions in a recorder with tone holes, *The Journal of the Acoustical Society of America*, **138**(2): 858–873, doi: 10.1121/1.4926902.

32. Yoshikawa S. (2000), A pictorial analysis of jet and vortex behaviours during attack transients in organ pipe models, *Acta Acustica united with Acustica*, **86**(4): 623–633.

33. Yoshikawa S., Tashiro H., Sakamoto Y. (2012), Experimental examination of vortex-sound generation in an organ pipe: A proposal of jet vortex-layer formation model, *Journal of Sound and Vibration*, **331**(11): 2558–2577, doi: 10.1016/j.jsv.2012.01.026.